Experiments on GOL-3 Multiple-Mirror Trap for Fusion Program

A.V. Burdakov[1,2], A. P. Avrorov[1], A.V. Arzhannikov[1,3], V.T. Astrelin[1,3], V.I. Batkin[1], A.D. Beklemishev[1,3], V.S. Burmasov[1,3], P.V. Bykov[1], L.N. Vyacheslavov[1,3], G.E. Derevyankin[1], V.G. Ivanenko[1], I.A. Ivanov[1,3], M.V. Ivantsivsky[1,2], I.V. Kandaurov[1], A.A. Kasatov[3], S.A. Kuznetsov[3], V.V. Kurkuchekov[1], K.N. Kuklin[1], K.I. Mekler[1], S.V. Polosatkin[1,2], S.S. Popov[1], V.V. Postupaev[1,3], A.F. Rovenskikh[1], S.L. Sinitsky[1,3], V.D. Stepanov[1], A.V. Sudnikov[3], Yu.S. Sulyaev[1], I.V. Timofeev[1,3], V.F. Sklyarov[2], N.V. Sorokina[2], A.A. Shoshin[1]

[1] Budker Institute of Nuclear Physics SB RAS, Novosibirsk, Russia
[2] Novosibirsk State Technical University, Novosibirsk, Russia
[3] Novosibirsk State University, Novosibirsk, Russia

E-mail contact of main author: A.V.Burdakov@inp.nsk.su

Abstract. The GOL-3 Multiple-Mirror Trap is an 11-m-long solenoid with axially-periodical (corrugated) magnetic field that consists of 52 magnetic corrugation cells with B_{max}/B_{min} = 4.8/3.2 T. Deuterium plasma of 10^{20}-10^{22} m^{-3} density is heated up to ~2 keV ion temperatures (at ~10^{21} m^{-3} density and confinement time ~1 ms) by a high power relativistic electron beam. The plasma heating and confinement in the trap are of essentially turbulent nature. In general, achieved plasma parameters support our vision of a multiple-mirror trap as the alternative path to a fusion reactor with $\beta \sim 1$ and 10^{21}-10^{22} m^{-3} plasma density. Project of a new linear trap with multiple-mirror plugs is in progress in BINP. Several new experiments in support of the fusion program based on linear machines are presented. The main physical and technical challenge to be solved is an increase of duration of the electron beam from the available ~10 μs up to ~1 ms and further. This step will require a significant decrease of power of the electron beam from ~20 GW down to steady-state-feasible 10-100 MW and an exploration of a new parameter space. An intense electron beam source of a new type, based on a gaseous arc plasma emitter, was developed. The first experimental results on injection of this beam at ~80 keV, 2-10 MW, 0.1-0.3 ms into ~3×10^{19} m^{-3} deuterium plasma are presented. Main physical task for the reported experiments was to reach quasi-stationary plasma conditions during the long-pulse beam injection.

1. Introduction

Experiments on the multiple-mirror trap GOL-3 are directed to development of the fusion reactor concept [1]. During the last years the several key physical phenomena (enhanced confinement, suppression of electron heat transport and other) that enable achievement of high plasma parameters were identified in the experiments [2]. Project of a new linear trap with multimirror end plugs based in particular on GOL-3 results is in progress in BINP [3]. The main problem to be solved by the new facility is the increase of the plasma sustainment time. New approach to a fusion reactor suggests application of a long pulse or continuous electron beam injection for control of the plasma turbulence and potential. Practical feasibility of the reactor will heavily depend on a level of required beam power.

An intense electron beam source of a new type, based on a gaseous arc plasma emitter, was developed and installed into the end expander tank of GOL-3. Activity on development of the required technology of long pulse electron beam generation was previously reported (see, e.g. [4]). The beam with the emission current density of up to 20 A/cm^2 was formed at ~100 kV

accelerating voltage. In the preliminary test experiments the beam with a pulse length in a range of 0.1-1 ms was transported down to a collector at a distance of 1.5 m in an axial magnetic field of 0.05 T. The maximum achieved beam power was ~10 MW.

The new beam considerably increased duration of the plasma heating. The plasma parameters reached a quasi-stationary state for the first time in GOL-3 history. Estimates by the theory [5,6] predicted good relaxation efficiency of the beam under current experimental conditions. On the other hand, the beam power was four orders of magnitude less than previously used beams from the U-3 [7] and U-2 [8] generators. Therefore we did not expected achieving the same plasma parameters as have been reported previously. In order to keep the beam-plasma interaction at a high enough level we decreased the density down to ~10^{20} m^{-3} and even at lowered density the temperature was in the order of 100 eV. At these conditions some important non-linear plasma processes cannot be studied with our current capabilities. Mainly it applies to processes of turbulent suppression of axial electron heat transport [9], fast heating of ions [10] and reduction of axial plasma expansion by the bounce instability [11]. Despite this the experiments with the new beam give us for the first time possibility of studying turbulent beam-heated plasma at stationary conditions.

This paper opens a separate research line in the physical program for GOL-3 that will be continued further. We plan to continue experimental campaigns with our traditional research line using ~20 GW, ~10 μs electron beam at higher plasma parameters also.

2. Source of a Long-Pulse Electron Beam

One of the key design issues related to the beam injector is a cathode that should be capable to emit 10-100 A/cm^2 with the total current up to ~1 kA with pulse duration in the ~1 ms range. The second challenge is an electrode structure that should enable extraction and acceleration of high-current high-brightness electron beam. Among different types of cathodes suitable for producing such a beam, the plasma cathode was chosen. Extraction and acceleration of a high-perveance electron beam with the required brightness was achieved in multiple-aperture electron optic system [4], where the total beam current is summed from currents of many beamlets. One more problem to be solved is the impact of backwards high-power plasma flow from the trap to the electron beam source and acceleration of ions in the diode.

Apart form the beam energy and the current density the beam-plasma interaction strongly depends on the beam quality. Therefore the beam energy spread in the diode should be minimized. Full computational optimization with the modified POISSON-2 code has been done for the geometry of individual beamlet electrodes. Algorithms for computation of shape of plasma boundaries in the low-temperature approximation of uniform emission from the surface were developed earlier for diodes with plasma electrodes [12].

Conditions of the electron beam formation at the source with the design parameters (100 kV, 1 kA, 100 μs or more) were determined with features that allow 100-fold compression of the beam by guiding magnetic field, see Fig. 1. Here the electron current density

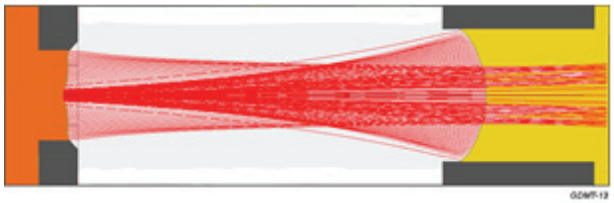

FIG. 1. Simulation of a beamlet in a single diode aperture. The left side is the cathode with a cathode plasma emitting electrons; the right one is the anode with an incoming plasma stream that emits ions.

averaged over the cathode aperture is 63 A/cm^2, the ion current density at the anode is ~1 A/cm^2, the diode current is 1.1 kA. The maximum pitch angle of electrons is ~0.07 rad. Guiding magnetic field is 0.05 T. In the numerical simulation of the diode exposed by the incident plasma flow a lossless motion of particles accelerated in the diode gap through the cathode and anode apertures without leaking to metal electrodes of the diode was achieved.

Layout of the generator of the long-pulse electron beam is shown in Fig. 2. It was installed in the (former) exit expander tank of GOL-3 replacing the output beam receiver that was previously used in experiments with the 200-kJ relativistic electron beam of the U-2 generator. General view of the electrodes is shown in Fig. 3. In the commissioning experiments the beam was dumped to a metal collector placed at different distances from the diode, typical shots are shown in Fig. 4. Detailed description of the system can be found in [13].

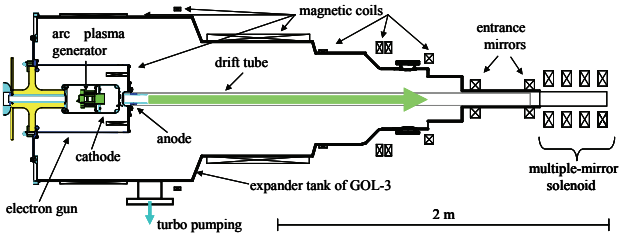

FIG. 2. Layout of the beam generator in GOL-3.

FIG. 3. General view of the electrodes.

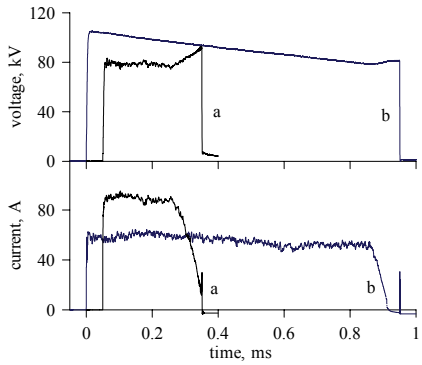

FIG. 4. Typical waveforms at operation with test receiver. Shots with 95 A current (a) and with ~0.9 ms duration (b) are shown. In both cases the beam was terminated by a preset shutdown of the arc plasma generator. Gradual voltage decrease is due to the discharge of HV capacitors.

3. Injection of the Long-Pulse Beam in GOL-3

After the commissioning of the beam generator was completed, experiments were started with the beam injection into the existing multiple-mirror confinement system. We should note here that the first task of the discussed experiments was to test-proof the technology of a long-pulse injection. Therefore no changes were made to the existing vacuum and magnetic structures of GOL-3. This decision resulted in a large distance from the diode to the first input magnetic mirror (that is referred to as the coordinate $z = 0$ further in the text) – see Fig. 2. Magnetic field gradually increases in the drift pass between the diode and the magnetic mirror, enabling thereby the adiabatic compression of the beam. The magnetic compression ratio in the experiments was varied from 12 to 210. Metal drift tube with several break gaps was inserted between the grounded anode and the high-field mirror area. This tube reduces electric fields in the drift space and influence vacuum conditions in the expander tank when operating with considerable gas flows from the main confinement section.

General layout of GOL-3 with the long-pulse electron beam generator is shown in Fig. **5**. The mean magnetic field in the multiple-mirror solenoid was 0.3-2 T. The plasma was created

from gas-puffed deuterium by the beam itself. Standard plasma creation system of GOL-3 turns to be not compatible with the first version of the long-pulse beam generator due to large gas and plasma flows that it produces towards the diode. Usually we used one central fast valve that gives the bell-shaped distribution like that shown in Fig. **5** (the dots are the readouts of fast vacuummeters and the solid line is the expected distribution).

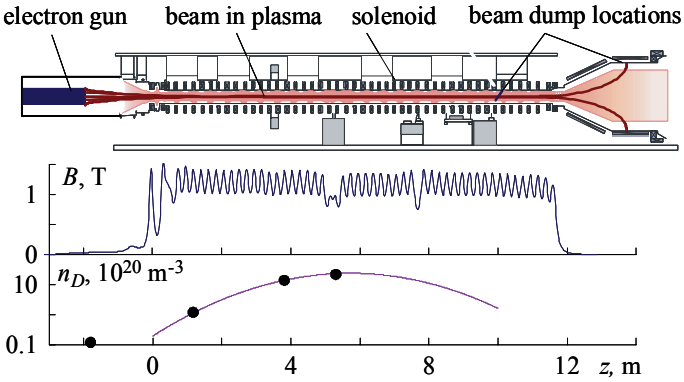

FIG. 5. Layout of the experiment. Axial profiles of magnetic field and initial gas density are shown.

The desired density distribution over the length was chosen by varying the initial gas pressure and triggering time for the valve. In these experiments the time delay between actuation of a fast valve and start of the beam injection was tenfold reduced comparing with our usual scenario in order to decrease gas load to the diode. The beam ionizes the gas within its cross-section during its transport through the device. The density dynamics in an observation point is determined by the balance between processes of local ionization of the puffed gas, the gas influx from the outside of the beam cross-section and plasma flow along the magnetic field. The beam occupied only small fraction of the gas-filled vacuum chamber, so charge exchange processes became very important for plasma confinement. Our further plans include replacing this gas-puffing technique with a special plasma gun that is under development now.

Magnetic field has 52 corrugation periods (cells of multimirror system) with 22 cm length. Mean magnetic field was from 0.3 to 1.8 T. The electron beam parameters were the following: the energy 70-100 keV, the beam current 15-100 A, the beam energy content up to 1 kJ, the pulse duration up to 300 μs, the beam power up to 10 MW. The initial current density was up to 20 A/cm^2.

After passing the plasma the beam was dumped either to a special tantalum collector that was placed at z = 10 m or to the walls of a beam shape transformer section of U-2 in weak magnetic field (decreasing therefore power loads to the wall). The magnetic field at position of the collector was significantly lowered usually comparing to the confinement section in order to decrease amount of back-scattered electrons and keep the heat loads at tolerable level, but it can be set as high as in the rest of solenoid if required.

The net current in the confinement section was measured in 8 different axial positions by Rogowski coils. Usually waveforms and amplitudes of the net currents practically coincided – see Fig. 6. This evidences that no current leaks to the wall were in the experiments. In most cases the net current was about

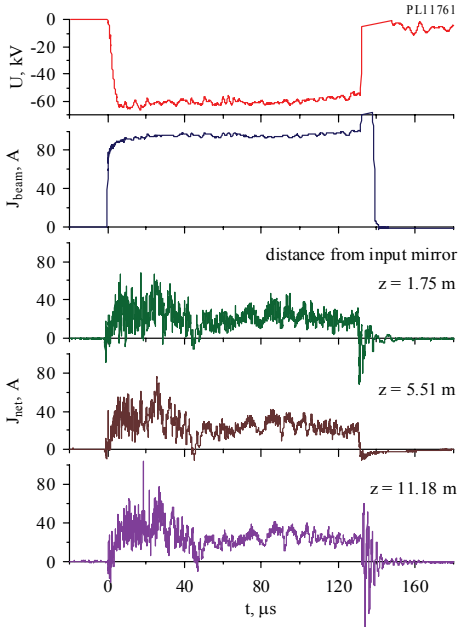

FIG. 6. Typical waveforms, top to bottom: accelerating voltage, current in the diode, net plasma currents at different coordinates z.

30-50% of the injected beam current (Fig. 6). As before with the relativistic electron beam [14], the beam current was partially neutralized by a counter flow of the return plasma current. Nevertheless a part of the beam could be lost in compression area between the diode and the input mirror.

Stability of the beam transport through the device was controlled with a special fast X-ray imaging camera that observed the tantalum beam collector. Figure 7 shows a typical X-ray image and its brightness profile. Size of the beam footprint is in a reasonable agreement with the expected value (see Fig. 8). Some expansion of the beam cross-section due to non-negligible gyro-radii of scattered beam electrons that have acquired large pitch-angles can be expected at lowest magnetic field.

The beam transport through the system was macroscopically stable. This is quite important because of close Kruskal-Shafranov limit at lowest magnetic fields. Some observed displacement of the beam center off the expected position was caused mainly by a non-ideality of the magnetic axis of the solenoid at low fields. Data from an array of Mirnov coils and from a fact CCD camera with 250 kHz frame rate indicate some MHD activity with fast rotation of magnetic perturbations in the middle section of the solenoid – Fig. 9. Nevertheless the displacements stayed at the safe level and did not affected the beam or plasma performance.

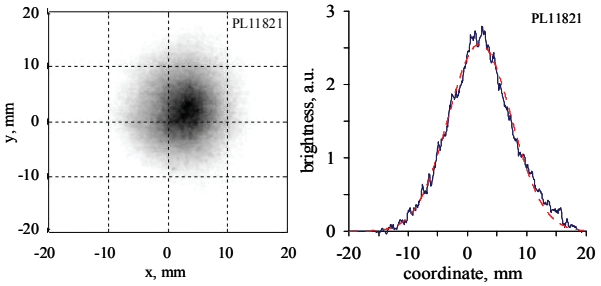

FIG. 7. Typical X-ray beam footprint at the collector after passing the 12-m-long plasma column. Mean B is 1.24 T. Gaussian fit is also shown by dashed line.

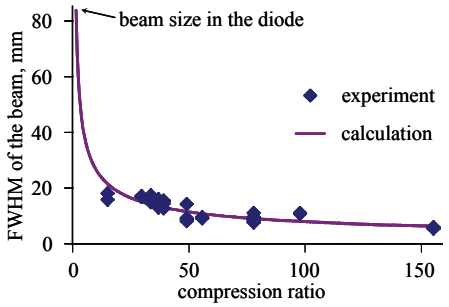

FIG. 8. Dependence of the X-ray beam footprint size on the magnetic compression ratio. Dots are the experiment; solid line is the expected value.

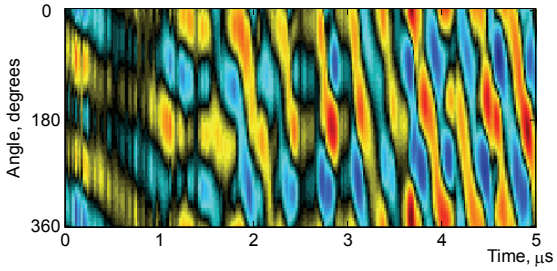

FIG. 9. Map of magnetic perturbations after the beam start in typical experiment.

4. Plasma Heating

Usually the most interesting part of plasma in a beam-plasma experiment is the entrance section where a beam is injected into a system. There the beam has minimal volume in the phase space and its interaction with plasma is the most intense. For this reason we relocate some plasma diagnostics to that end of the solenoid where the long-pulse beam was injected. The double-pulse Thomson scattering system was placed in the closest available port at z = 0.84 m, sharing this position with microwave diagnostics. New 280 GHz interferometer was at z = 3.04 m; hard X-ray detectors were at z = 0.45, 0.95 and 11.36 m; fast CCD cameras were at z = -0.43, 0.84 and 9.6 m (the first one observed the beam during magnetic compression in the drift section); fast video camera was at z = 4.18 m; soft X-ray detector was at z = 0.95 m. Other standard diagnostic instrumentation was also active, including distributed sets of diamagnetic and Mirnov coils, VUV detectors, Rogovsky coils, *etc*.

The beam injection into gaseous deuterium leads to its ionization and then to heating of the plasma. Typical waveforms for the shot with the beam power 1.7 MW are shown in Fig. 10. After the beam start there is some transition period where buildup of plasma occurs. Most part of the beam injection passes at the quasi-stationary conditions. The net current stays almost at the same fraction of the beam current during the shot. Power of the bremsstrahlung from the beam collector follows the beam current. This means that degree of the beam relaxation in the plasma stays practically the same during the shot.

In these experiments we use a dedicated microwave diagnostics suitable for detection of radiation at double plasma frequency [15]. Such radiation is a good indicator of a high-level non-linear Langmuir turbulence that is pumped by the beam during its relaxation in plasma. This signal lasts for most part of the shot in Fig. 10, its spectrum is shown in Fig. 11. At the beam current of ~25 A and the magnetic field of 1.24 T the specific power achieves ~100 W/cm at 94 GHz (assuming isotropic emission). This corresponds to ~1% of the total electron beam power taking into account ~1 m axial length of the emission zone.

Closer to the end of the beam injection observed VUV emission starts rising. This can be caused by local density growth that also leads to changes to the beam-plasma interaction regime and to decrease of the microwave intensity. As is usual for a beam-plasma experiment, population of suprathermal electrons is observed by soft X-ray emission from the plasma. Soft X-ray power and corresponding density (and/or mean energy) of fast electrons degrade with the increase of the density. Soft X-ray detector is placed closer to the beam input in the high-density-gradient zone (see Fig. 5), so the density growth starts earlier there. The bottom waveform in Fig. 10 is raw interferogram at 280 GHz; this signal is shown as the reference only because the plasma diameter in this case was close to diameter of the probing beam. Albeit the interferometer stands in the middle part of GOL-3, a trend of density growth is noticeable during the late part of the shot.

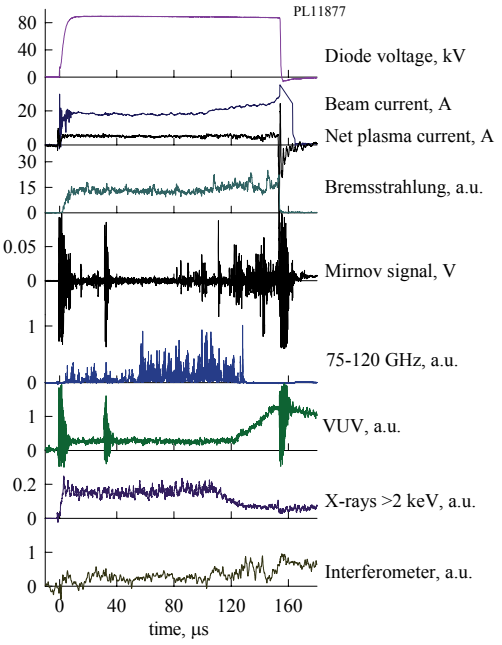

FIG. 10. Waveforms for 1.7 MW shot. Operating mode is $n_e \sim (0.5\text{-}0.9)\times10^{20}$ m^{-3}, $\langle B\rangle = 1.24$ T.

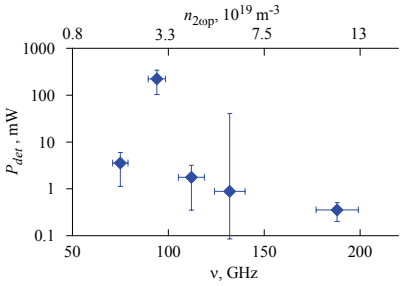

FIG. 11. Spectrum of microwave emission at 20-25 A beam current. Upper axis shows plasma density that gives the same double plasma frequency.

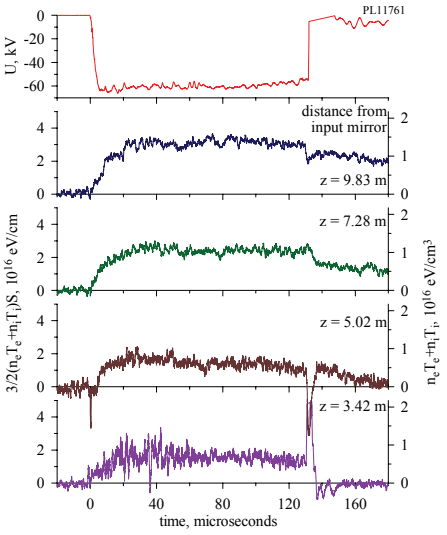

FIG. 12. Diamagnetism of the plasma at different coordinates. Operating mode is $n_e \sim (0.5\text{-}0.9)\times10^{20}$ m^{-3}, $\langle B\rangle = 0.31$ T.

The plasma pressure starts growing after start of the beam injection. Depending on the parameters, this phase lasts for 15-30 μs. Then the plasma pressure stays at the quasistationary level. The pressure distribution over the length is almost uniform (see Fig. 12). This strongly differs these experiments from the best regimes with high-power relativistic beams in GOL-3 (e.g. [7,8]) and in earlier 50-ns-scale experiments [16], where the heating was accented near the beam injection point. Probably the cause is plasma existing between the diode and the input mirror that interacts with the beam and therefore worsens the beam phase space before it enters the confinement zone. After the beam injection terminates, diamagnetic and soft X-ray signals last for up to 1 ms (see Fig. 13) that indicates slow decay of trapped high-energy electrons.

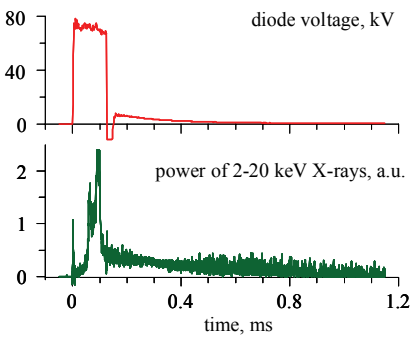

FIG. 13. Waveforms of the diode voltage (top) and of soft X-ray emission power in 2-20 keV interval (bottom). Tail of the X-ray signal lasts for ~1 ms.

Typical diamagnetic mean energy of an electron-ion pair is 100-150 eV. Electron temperature is up to 20-70 eV by Thomson scattering. The rest of the plasma energy is carried by the suprathermal electrons mostly, because estimates of ion temperature are quite low. In some shots Thomson scattering data deviates from a Maxwellian distribution, see Fig. 14. Radial density profile is quite uniform according to Thomson measurements that give up to 6 radial pints in each shot at z = 0.84 m where this system is located (Fig. 15).

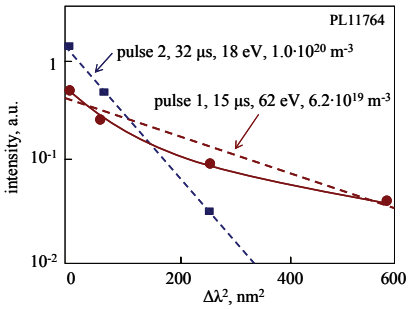

FIG. 14. Typical Thomson scattering spectra for 7 MW, 75 keV shot. Spectrum in pulse 1 at 15 μs exhibits signs of non-Maxwellian electron distribution function (shown by the solid line). Pulse 2 was performed at 32 μs shortly after termination of the beam injection. Maxwellian fits are shown by dashed lines.

5. Summary and Discussion

We started a new line in the experimental program of GOL-3. Emphasis is made on non-relativistic electron beam of a moderate power and long pulse length. The new technology of high-power electron beams suitable for injection into the trap for plasma heating is developed. The electron beam gun based on the plasma emitter and the multi-aperture diode was integrated into the multiple-mirror trap GOL-3.

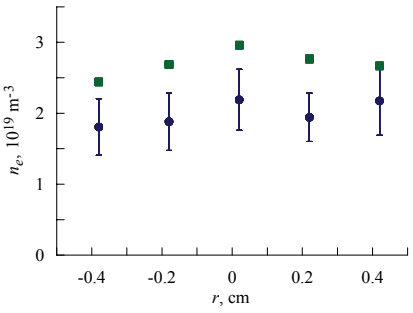

FIG. 15. Radial profiles of electron density by Thomson scattering at 25 μs (dots) and 60 μs (squares) after beginning of the beam injection. The error bars (shown for t = 25 μs only) include shot-to-shot spread.

Beam compression by the magnetic field (up to 200-fold) and its stable transportation in the 15-meter-long trap was demonstrated at ~100 A, 100 keV, 0.1-0.5 ms. Plasma heating by the beam at 10^{19}-10^{21} m^{-3} density was observed by several diagnostics. The beam duration allows us to study plasma properties in a quasistationary state for the first time in GOL-3. A non-Maxwellian distribution functions of plasma electrons were observed; this is usual for beam-plasma experiments. Further plans include an upgrade of the beam generator, a new source of preliminary plasma and an upgraded NBI system.

Acknowledgments

This work was financially supported by Ministry of Education and Science RF, by Grant No. 11.G34.31.0033 of the Russian Federation Government, by Presidium RAS program 30, by RFBR projects 10-02-01317a, 10-08-00707a, 11-01-00249a, 11-02-00563a, by Council of the Russian Presidential Grants project NSh-7792.2010.2.

References

[1] BURDAKOV, A. V., et al., "Concept of Fusion Reactor Based on Multi-Mirror Trap", Fusion Sci. Technol., **59** (No 1T) (2011) 9.

[2] BURDAKOV, A. V., et al., "Status and Prospects of GOL-3 Multiple-Mirror Trap", Fusion Sci. Technol., **55** (No. 2T) (2009) 63.

[3] BEKLEMISHEV, A. D., et al., "Novosibirsk Project of Gas-Dynamic Multiple-Mirror Trap", Open Magnetic Systems for Plasma Confinement (Proc. 9th Internat. Conf. Tsukuba, 2012), paper I-5, *to be published in* Fusion Sci. Technol., **63** (2013).

[4] KANDAUROV, I., et al., "Submillisecond Electron Beam for Plasma Heating in Multi-Mirror Trap GOL-3", Fusion Sci. Technol., **59** (No. 1T) (2011) 67.

[5] TIMOFEEV I. V., TEREKHOV, A. V., "Simulations of Turbulent Plasma Heating by Powerful Electron Beams", Phys. Plasmas, **17** (2010) 083111.

[6] TIMOFEEV, I. V., "Two-Dimensional Simulations of Nonlinear Beam-Plasma Interaction in Isotropic and Magnetized Plasmas", Phys. Plasmas, **19** (2012) 042108.

[7] BURDAKOV, A. V., et al., "Experiments on the Collective Interaction of a Microsecond Relativistic Electron Beam with a Plasma in the GOL-3 Facility", J. Exper. Theor. Phys., **82** (1996) 1120.

[8] AGAFONOV, M. A., et al., "Plasma Heating by High-Energy-Content Microsecond Electron Beam at GOL-3-II Facility", Plasma Phys. Contr. Fusion, **38** (No.12A) (1996) A93.

[9] ASTRELIN, V. T., et al., "Generation of Ion-Acoustic Waves and Suppression of Heat Transport during Plasma Heating by an Electron Beam", Plasma Phys. Rep., **24** (1998) 414.

[10] ARZHANNIKOV, A. V., et al., "Dynamics of Ions of a Beam-Heated Plasma in a Cell of Multimirror Open Trap", Fusion Sci. Technol., **43** (No. 1T) (2003) 172.

[11] BEKLEMISHEV, A. D., "Bounce Instability in a Multi-Mirror Trap", Fusion Sci. Technol., **51** (No. 2T) (2007) 180.

[12] ASTRELIN, V. T., et al., "Numerical Simulation of Diodes with Plasma Electrodes", High Current Electronics (Proc. 15th Internat. Symp. Tomsk, 2008), (2008) 11.

[13] KURKUCHEKOV, V. V., et al., "Novel Injector of Intense Long Pulse Electron Beam for Linear Plasma Devices", Open Magnetic Systems for Plasma Confinement (Proc. 9th Internat. Conf. Tsukuba, 2012), paper P-19, *to be published in* Fusion Sci. Technol., **63** (2013).

[14] POSTUPAEV, V. V., et al., "Role of q Profile for Plasma Confinement in the Multimirror Trap GOL-3", Fusion Sci. Technol., **47** (No.1T) (2005) 84.

[15] ARZHANNIKOV, A. V., et al., "Diagnostic system for studying generation of subterahertz radiation during beam-plasma interaction in the GOL-3 facility", Plasma Phys. Rep., **38** (2012) 450.

[16] ARZHANNIKOV, A. V., et al., "New Experimental Results on Beam-Plasma Interaction in Solenoids", Plasma Phys. Contr. Fusion, **30** (1988) 1571.